CORROSION SCIENCE AND TECHNOLOGY, Vol.12, No.4(2013), pp.163~170

Determining Factors for the Protectiveness of the Passive Film of FeCrN Stainless Steel Formed in Sulfuric Acid Solutions

Heon-Young Ha[1,†] and Tae-Ho Lee[1]

[1]*Advanced Metallic Materials Division, Korea Institute of Materials Science, 797 Changwondaero, Seongsangu, Changwon, Gyeongnam, 642-831, South Korea*

(Received July 1, 2013; Revised July 15, 2013; Accepted July 16, 2013)

In NaCl solutions acidified with H_2SO_4, Fe20Cr1.1N alloy showed enhanced pitting corrosion resistance than Fe20Cr alloy. An XPS analysis revealed that the passive film of Fe20Cr1.1N alloy contained higher cationfraction of Cr than that of Fe20Cr alloy, and nitrogen was incorporated into the film. In addition, it was found that the passive film of Fe20Cr1.1N alloy was thinner and had higher oxygen vacancy density than that of Fe20Cr alloy. Based on these observations, it was concluded that the chemical composition was the determining factor for the protectiveness of the passive film of Fe20Cr based alloy in dilute H_2SO_4 solution.

Keywords : *stainless steel, nitrogen, sulfuric acid solution, passive film, Mott-Schottky, XPS*

1. Introduction

It is widely agreed that the nitrogen as an alloying element enhances the pitting corrosion resistance of stainless steels, and the mechanism for the positive effect of nitrogen has been extensively investigated.[1-9] The dissolved nitrogen in stainless steel is reported to change the physical, chemical and electronic properties of the passive film, and many attempts have been made to correlate the changed properties with the passive film protectiveness.[1,3,7,9-12] A consensus exists in the fact that the alloyed nitrogen changes the chemical composition and chemical structure of the passive film, which includes the increase in the cation fraction of chromium and nitrogen enrichment on the film-metal interface or its incorporation into the film.[1,3,7,9-12] The nitrogen effect of increasing the Cr content in the passive film formed on the nitrided stainless surface was reported by Willenbruch,[13] and the same phenomenon was observed in the passive film of Fe20Cr1.1N alloy formed in a borate-phosphate buffer solution.[11] In addition, Olefjord[9] provided the evidence of nitrogen-enrichment on the film-metal interface during a passivation of Fe20Cr20Ni6Mo (0.011, 0.19) N alloys in an acidified chloride solution. Vanini[10] also reported the nitrogen-enrichment on the film-metal interface of Fe17Cr13Ni0.15N alloy, and Olsson[14] observed that phenomenon on the passive film of 2205 duplex stainless steel-containing 0.2 wt% of nitrogen. As for the physical properties of the passive film, Olefjord[9] reported that the passive film thickness was not affected by nitrogen alloying in the Fe20Cr20Ni6Mo (0.011, 0.19) N which was formed in the 0.1 M HCl+0.4 M NaCl solution although the pitting corrosion resistance was increased by nitrogen addition. However, Fu[15] observed the increased thickness in the passive film of Fe19Cr19Mn2Mo0.96N alloy formed in 0.5 M H_2SO_4+0.5 M NaCl solution. Besides the physico-chemical properties, electronic properties of the passive film were frequently investigated to evaluate the protectiveness of the film.[11,16,17] The relationship between the decrease in the defect density (that is, oxygen vacancy concentration) and the enhancement of the pitting corrosion resistance was observed in Fe21Cr13Ni5Mn2Mo2.47N alloy[16] and nitrogen-bearing 316L type stainless steel[17]. Additionally, increase in the 2nd donor density (that is, Cr^{6+} concentration) in the passive film was reported to be responsible for the stable passivity of nitrogen-bearing Fe20Cr alloy.[11] As listed above, the effect of nitrogen on the passive film properties appears in various aspects, and it is needed to find out which is the most important factor determining the passive film protectiveness of nitrogen-bearing stainless steel. Therefore, in this paper, the various properties of the passive films of Fe20Cr and Fe20Cr1.1N alloys formed in H_2SO_4 solution were investigated in terms of physical, chemical, and electronic structure, and the determining factor in the passive film protectiveness was proposed.

† Corresponding author: hyha2007@kims.re.kr

2. Experimental

2.1. Materials and electrodes

Investigated alloys were Fe20Cr (Fe-19.82Cr in wt%) and Fe20Cr1.1N (Fe-20.64-1.07N in wt%) alloys. Fe20Cr alloy was produced using a vacuum arc melting furnace. The sample was homogenized at 1200 °C for 100 minutes and hot rolled into plates of 3 mm thick. The hot rolled plate was solution annealed at 1050 °C and water quenched. Fe20Cr1.1N alloy was produced using a pressurized induction melting furnace under N_2 partial pressure of 15 bar. After homogenization at 1250 °C for 2 hours, the ingot was hot rolled into a plate of 4 mm thick, and the plates were solution annealed at 1200 °C for 2 hours followed by water quenching. Fe20Cr1.1N alloy was confirmed to have a single austenite phase with a super-saturated nitrogen, and no precipitation was observed. For the electrochemical tests, the samples were mounted in an epoxy resin and mechanically ground to #2000 using a SiC paper. For the XPS analysis, the samples were polished to 1 μm using a diamond suspension. The exposed area for the electrochemical test was controlled to be 0.13 cm^2 using electroplating tape.

2.2. Electrochemical tests

Electrochemical tests were carried out using a three-electrode cell, and a saturated calomel reference electrode (SCE) and a Pt plate for a counter electrode were used. The electrochemical signal was monitored using a Reference 600 (GAMRY) potentiostat.

Pitting corrosion resistance of the alloys was evaluated using a potentiodynamic polarization test in the 0.2 M chloride solutions with 0-0.05 M H_2SO_4 at a scan rate of 3 mV s^{-1}. In order to reduce severe active dissolution during the polarization test in highly acidic solution (e.g., 0.2 M NaCl+0.05 M H_2SO_4 solution), the relatively fast potential sweep rate was chosen. Then, the protectiveness of the passive film was investigated in various angles. An XPS analysis was carried out to examine the film thickness and chemical structure of passive films of Fe20Cr and Fe20Cr1.1N alloys, which were grown in a deaerated 0.005 M H_2SO_4 solution by applying 0.3 V_{SCE} for 4 hours. XPS measurement was performed using an ESCALab 250 spectrometer with an Al kα anode X-ray source (150 W, 15 kV, hv=1486.6 eV). The nitrogen effect on the passive film thickness examined by the XPS was verified again by galvanostatic reduction test. In a deaerated 0.0005 M H_2SO_4 solution, the passive films were potentiostatically formed at -0.2 V_{SCE} and 0.3 V_{SCE} for 30 minutes, and then the films were reduced by applying constant cathodic current density of -10 μAcm^{-2}. From the consumed charge during the cathodic reduction of the oxide film, the passive film thickness was calculated.[18-20] Lastly, donor density (N_D) of the passive film was obtained from Mott-Schottky analysis. The two alloys were passivated in a deaerated

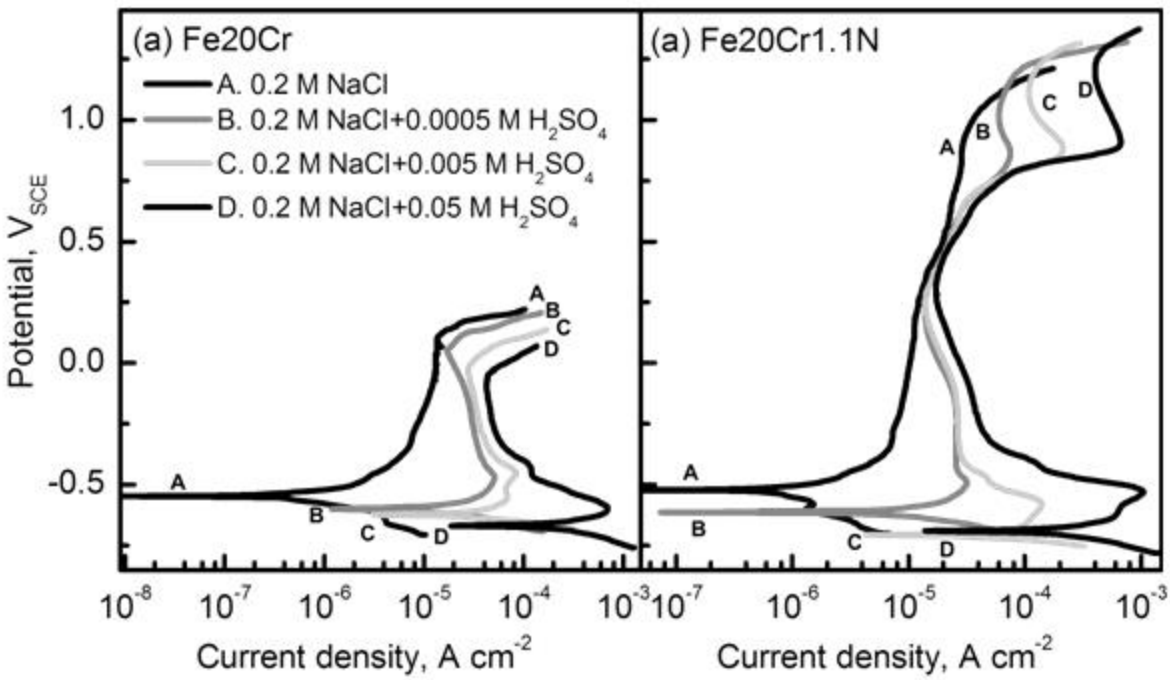

Fig. 1. Polarization curves of Fe20Cr and Fe20Cr1.1N alloys measured in deaerated 0.2 M NaCl solution with various concentrations of H_2SO_4 (20 °C) at a potential sweep rate of 3 mV s^{-1}.

0.1 M H_2SO_4 solution by applying 0.38 V_{SCE} for 4 hours, and then the capacitance was measured by sweeping the applied potential in the negative direction from the film formation potential to -0.46 V_{SCE}, while simultaneously imposing a small amplitude sinusoidal voltage perturbation of 10 mV (peak-to-peak) at a frequency of 1000 Hz. Before each electrochemical test, the working electrode was cathodically reduced at -1.0 V_{SCE} for 300 seconds to reduce an air-formed oxide.[20-21] Test solutions were deaerated by N_2 purging and solution temperature was maintained at 20°C. The polarization test, the galvanostatic reduction test and the Mott-Schottky analysis were performed at least 3 times, and good reproducibility was confirmed.

3. Results and Discussion

Fig. 1 shows polarization curves of the two alloys measured in deaerated 0.2 M NaCl solutions with various concentrations of H_2SO_4. In all solutions, pitting corrosion did not occur in Fe20Cr1.1N alloy while it took place in Fe20Cr alloy, which confirmed the higher resistance against the pitting corrosion of nitrogen-bearing alloy.[1,3,7] As pH decreased, that is H_2SO_4 concentration increased, a critical dissolution current density level increased and a corrosion potential level lowered in both alloys. Additionally, the pitting potential level of Fe20Cr alloy decreased as the solution pH decreased (Fig. 1(a)). However, it was noted that the lowest passive current density of Fe20Cr1.1N alloy measured at approximately 0.3 V_{SCE} was not significantly affected by the solution pH.

The pH levels of the simple 0.2 M NaCl solution without H_2SO_4 and 0.2 M NaCl solution with 0.0005 M H_2SO_4 were 6.13 and 3.01, respectively. In these neutral and mild acid solutions, Fe20Cr and Fe20Cr1.1N alloys were passivated below their corrosion potential level, and hence the two alloys did not show the active-passive transition behavior. Meanwhile, in the strong acid solutions with a lower pH level than 2.5 (0.2 M NaCl solution containing 0.005-0.05 M H_2SO_4), the alloys clearly exhibited the active-passive transition as concretely discussed in the reference.[21] Defining the active and passive state of Fe20Cr and Fe20Cr1.1N alloy is important to determine the passivation potential for the subsequent experiments.

Fig. 1 clearly presents that the solutionized nitrogen is beneficial to the enhancement of the resistance to pitting corrosion of Fe20Cr-based alloy, and this result was observed in the acidified chloride solution with H_2SO_4 regardless of the solution pH. In order to understand the reason for the promoted pitting corrosion resistance of Fe20Cr1.1N alloy, the characteristics of the passive film was closely investigated. Firstly, a thickness and a chemical structure of the passive film were investigated by an XPS analysis. The film was formed in deaerated 0.005 M H_2SO_4 solution (pH 2.07) by applying a constant anodic potential of 0.3 V_{SCE} for 4 hours, at which the lowest passive current density appeared. Fig. 2 shows the chemical composition depth profiles of the passive films of the alloys. The passive films of Fe20Cr and Fe20Cr1.1N alloys formed in a dilute H_2SO_4 solution were mainly composed of Cr, Fe and O. In both alloys, Fe content at the film surface was as low as 4 at%, and it gradually increased to approximately 80 at%. In addition, Cr content in the passive film was higher than that in the matrix, and its maximum value was approximately 30 at%, which was shown at approximately 0.5 nm point from the film surface. Appreciable amount of nitrogen was detected in the passive film of Fe20Cr1.1N alloy, whose maximum value reached up to 5.44 at% at the film-metal interface. It was worth mentioning that the passive film of Fe20Cr1.1N alloy had higher Cr cation fraction ([Cr]/[Fe+Cr]) than that of Fe20Cr alloy (Fig. 2(c)). At the film surface, the Cr fraction value

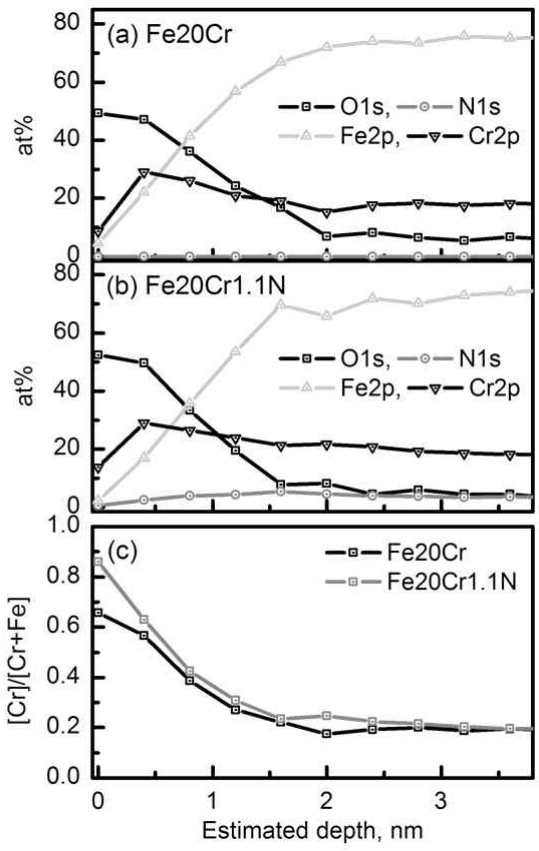

Fig. 2. Chemical composition depth profiles of the passivated surface of (a) Fe20Cr and (b) Fe20Cr1.1N alloys. (c) Depth profiles of the cation fraction of Cr ([Cr]/[Fe+Cr]). The passive films were potentiostatically grown in deaerated 0.005 M H_2SO_4 solution (20 °C) by applying constant potential of 0.3 V_{SCE} for 4 hours.

reached as high as 0.87 for Fe20Cr1.1N alloy and 0.66 for Fe20Cr, respectively. The high Cr fraction over 0.5 at the film surface demonstrates that the passive film surface is mainly composed of Cr_2O_3, due to the higher solubility of Fe than Cr in H_2SO_4 solution.[21,22] The composition depth profiles of O and Cr shown in Fig. 2 also provide the information for the thickness of the passive film. The film-metal interface of Fe20Cr alloy was located at approximately 2.0 nm from the surface, while that of Fe20Cr 1.1N alloy was at approximately 1.6 nm. The estimated film thickness based on Fig. 2 was further supported by the binding energy spectra of O_{1s} (Fig. 3(a) and 3(b)) and Cr_{2p} (Fig. 3(c) and 3(d)). Fig. 3(a) and 3(b) shows two distinguishable peaks located at 530.4 eV and 532.0 eV, which correspond to the binding energy of O^{2-} (oxide) and OH^- (hydroxide),[9,14,23] respectively. The OH^- peak at 532.0 eV appeared only at the film surface. Fig. 3(a) and 3(b) show that the binding energy intensity of O_{1s} more rapidly decreases in Fe20Cr1.1N alloy than that of Fe20Cr alloy with increasing in the sputtered depth. After the 4th sputtering cycle (1.6 nm from the surface) of the passivated surface of Fe20Cr1.1N, O^{2-} peak at 530.4 eV almost diminishes, while that for Fe20Cr alloy is still distinguishable. The binding energy spectra of Cr_{2p} also support this observation. Fig. 3(c) and 3(d) show two peaks at 574.2 eV and 576.4 eV which correspond to Cr^0 (metal) and Cr^{3+} (oxide), respectively.[23,24] As sputtering proceeded, the Cr^{3+} (oxide) peak decreased and Cr^0 (metal) peak increased. Comparing of Fig. 3(c) with 3(d), the retarded decrease in the intensity of the peak at 576.4 eV (Cr^{3+} (oxide)) is observed in the passivated surface of Fe20Cr alloy. From the O_{1s} and Cr_{2p} binding energy spectra, it is con-

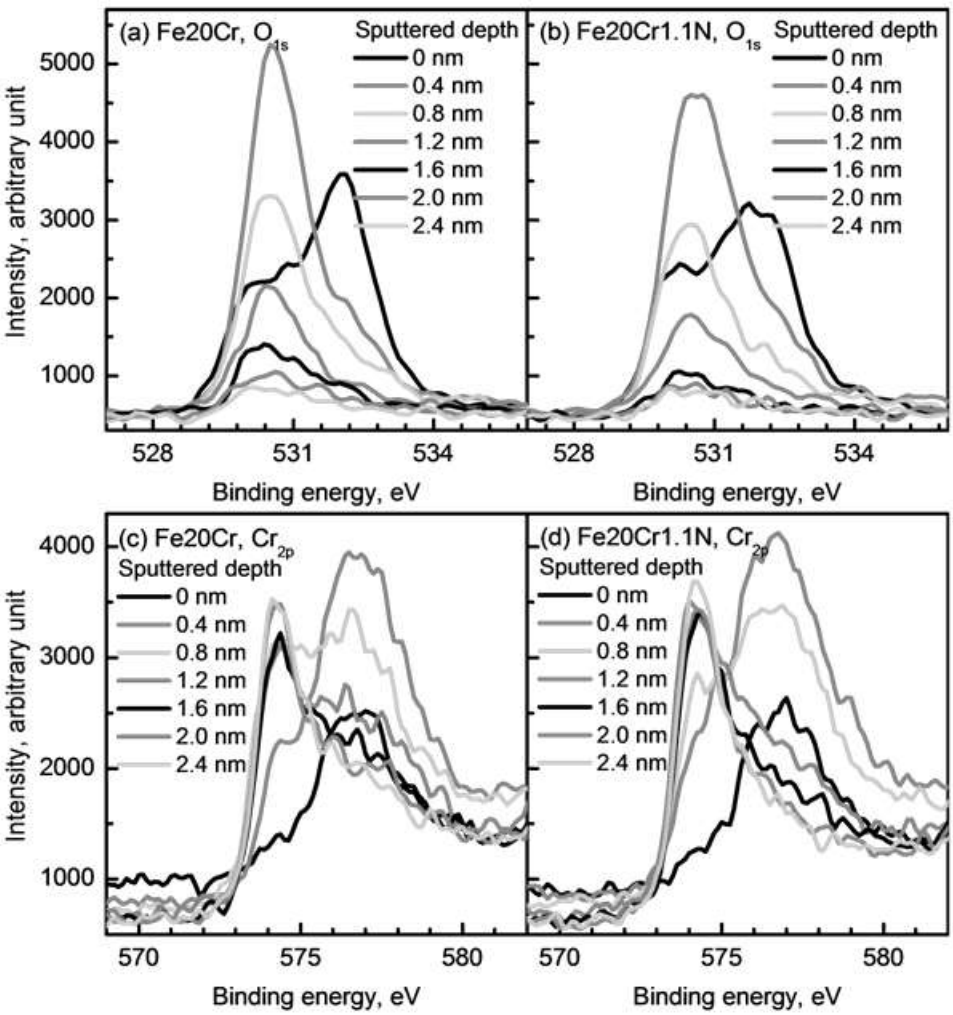

Fig. 3. Binding energy spectra of (a) O_{1s} and (c) Cr_{2p} in the passivated Fe20Cr alloy, and those of (b) O_{1s} and (c) Cr_{2p} in the passivated Fe20Cr1.1N alloy. The passive films were potentiostatically grown in deaerated 0.005 M H_2SO_4 solution (20 °C) by applying constant potential of 0.3 V_{SCE} for 4 hours.

firmed that the film-metal interface of Fe20Cr was located at approximately 2.0 nm from the surface and that for Fe20Cr1.1N was estimated to be 1.6 nm.

As for the nitrogen-bearing alloy, the evidences of the nitrogen incorporation into the passive film and the nitrogen enrichment on the film-metal interface are clearly found in Fig. 4. Fig. 4(a) and 4(b) show the binding energy spectra of N_{1s} at the film surface and matrix of Fe20Cr and Fe20Cr1.1N alloy, respectively. While no discriminable peak was observed in the binding energy spectra of the passivated surface on Fe20Cr alloy without nitrogen, the distinctive N_{1s} peak appeared in the passive film and the matrix of Fe20Cr1.1N alloy. The binding energy spectra of N_{1s} were divided into two peaks located at 369.9 eV and 397.7 eV. The 369.9 eV is known as the binding energy of Cr-N bonding,[3,9,11,13,25] and 397.7 eV isreported to correspond to the binding energy levels of Cr-N bonding[3,10,13] or Cr_2N nitrides.[9,25] As described in Fig. 2 and 3, the film thickness of Fe20Cr1.1N alloy was approximately 1.6 nm, and Fig. 4(b) presents that the N_{1s} peak with the highest intensity appears at the 1.6 nm depth point from the surface. Fig. 4(c) clearly shows that the incorporation of nitrogen into the film and the nitrogen-enrichment at the film-metal interface as well. In summary, the XPS analyses on the passive films of the alloys formed in dilute H_2SO_4 solution showed that both chromium and nitrogen concentrations increased in the passive film because of nitrogen alloying in the Fe20Cr alloy matrix, and thinner passive film was formed on the nitrogen-bearing Fe20Cr alloy.

The thinner passive film formation on Fe20Cr1.1N alloy than that of Fe20Cr alloy was confirmed again by an electrochemical test. Galvanostatic reduction test was conducted on the passive films of the alloys, which were formed in 0.0005 M H_2SO_4 solution (pH 3.04) by applying constant passivation potential. Fig. 5(a) shows polarization curves measured in the H_2SO_4 solution at a scan rate of 3 mV s^{-1}. In acid solutions above the pH level of approximately 3, both alloys were passivated below their corrosion potential levels.[21] For this reason, -0.2 V_{SCE} and 0.3 V_{SCE} were chosen as passivation potentials based on Fig. 5(a), and the passive films were potentiostatically grown at the determined potential levels for 30 minutes. Then, the films were galvanostatically reduced by applying a constant cathodic current density of -10 μA cm^{-2}. Fig. 5(b) and 5(c) show the potential transition profiles against time conducted on the passive films formed at -0.2 V_{SCE} and 0.3 V_{SCE}, respectively. By applying the cathodic current density, the passive oxide films are reduced via the following reaction; $(Fe, Cr)_2O_3 + 6H^+ + 2e^- \rightarrow 2(Fe, Cr)^{2+} + 3H_2O$,[18] and consequently the potential measured on the passivated metal surface decreases until reaching the stable potentiallevel. When the potential reaches the stable potential, the passive oxide layer can be considered to be fully reduced. The important result obtained from this test is the fact that the passive film of nitrogen-bearing alloy could be fully reduced with consuming less cathodic charge than that of Fe20Cr alloy without nitrogen. From the consumed charge during the reduction, which was directly converted from the current applying time, the thickness of the passive film could be calculated.[18,19] Assuming the reduction efficiency was 100 % because the test solution was mild acid solution with a pH 3.04,[26,27] the passive film thickness was calculated using materials constants (passive film molecular weight ($M_{(Fe,Cr)2O3}$= 155.84 g mol^{-1}, and passive film density ($\rho\gamma_{-(Fe,\ Cr)2O3}$) = 5.23 g cm^{-3}). The calculated passive film thickness is displayed in Fig. 5(d). The film of Fe20Cr alloy formed at -0.2 V_{SCE} had a thickness of 0.67 nm and that formed at 0.3 V_{SCE}

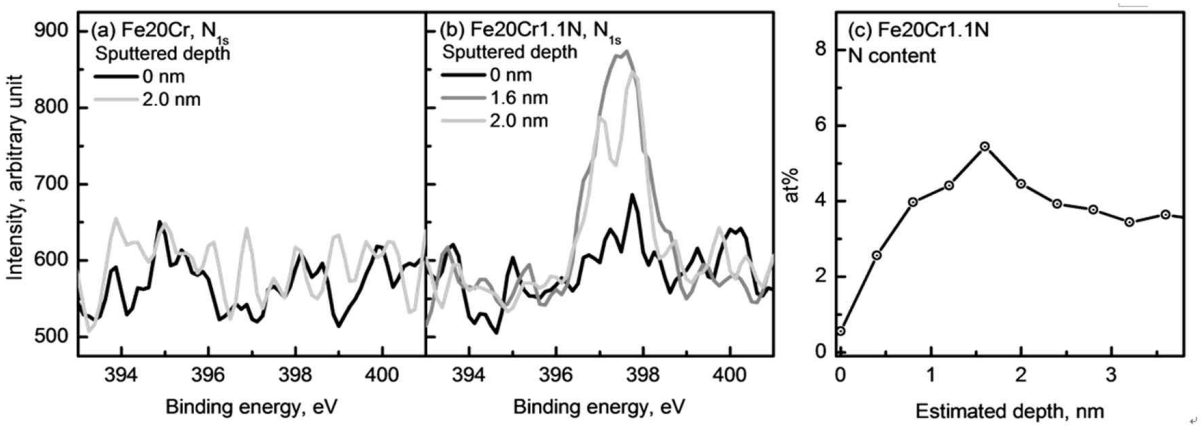

Fig. 4. Binding energy spectra of N_{1s} in the passivated surface of (a) Fe20Cr and (b) Fe20Cr1.1N alloys. (c) Chemical composition depth profile of N in the passivated surface of Fe20Cr1.1N alloy. The passive films were potentiostatically grown in deaerated 0.005 M H_2SO_4 solution (20 °C) by applying constant potential of 0.3 V_{SCE} for 4 hours.

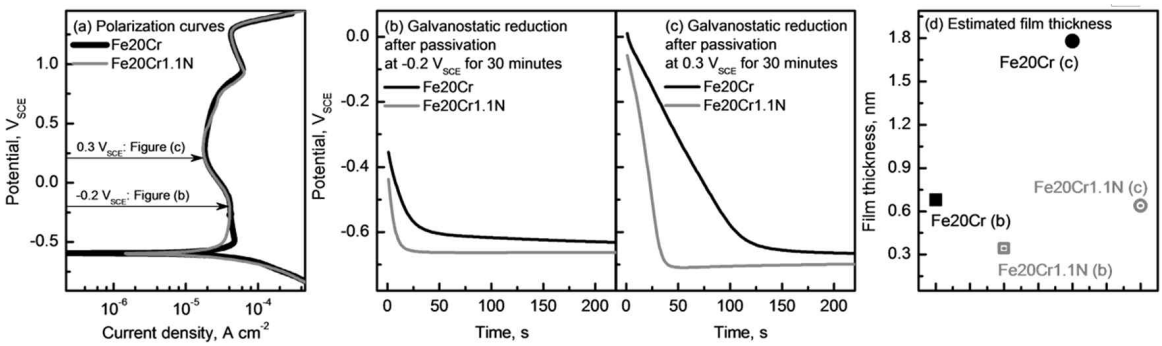

Fig. 5. (a) Polarization curves of Fe20Cr and Fe20Cr1.1N alloys measured in deaerated 0.0005 M H_2SO_4 solution (20 °C) at a potential sweep rate of 3 mV s^{-1}. Potential transition curve during the galvanostatic test by applying constant cathodic current density of -10 μA cm^{-2} of the alloys after passivation (b) at -0.2 V_{SCE} for 30 minutes and (c) at 0.3 V_{SCE} for 30 minutes. (d) Film thickness of the alloys calculated from the galvanostatic test results.

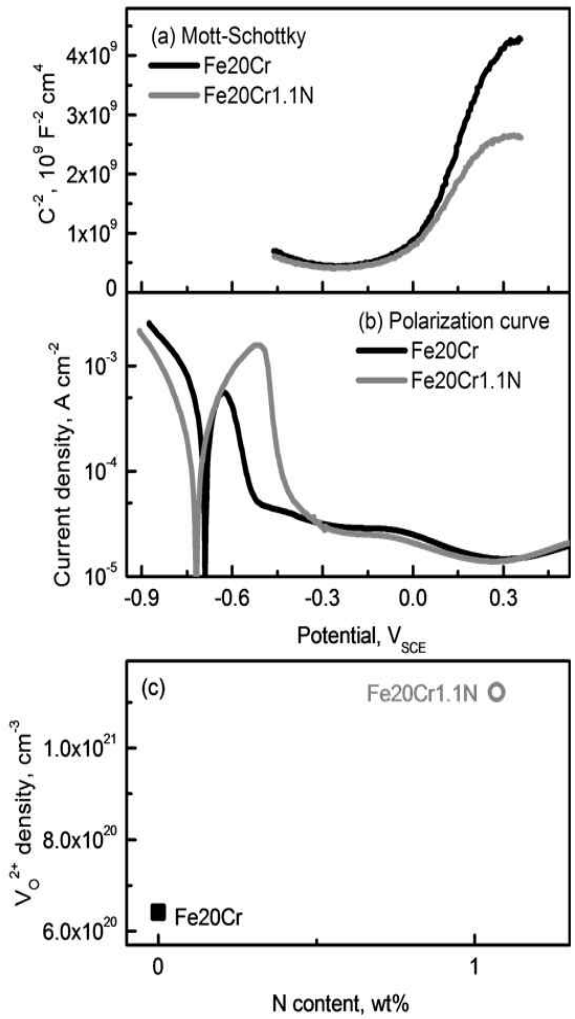

Fig. 6. (a) Mott-Schottky plots of Fe20Cr and Fe20Cr1.1N alloys measured in deaerated 0.1 M H_2SO_4 solution (20 °C, 1000 Hz, ±10 mV). (b) Polarization curves of the alloys measured the same solution at a potential sweep rate of 3 mV s^{-1}. (c) Donor density of the alloys calculated from the Mott-Schottky analysis.

was 1.77 nm. In presence of nitrogen in the Fe20Cr matrix, the film thickness was calculated to be 0.34 nm at -0.2 V_{SCE}, and 0.63 nm at 0.3 V_{SCE}, respectively. In both cases, the passive film of Fe20Cr1.1N alloy appeared to be thinner than that of Fe20Cr alloy, and this result supported the XPS results in Fig. 2.

As mentioned in the introduction section, the relationship between the semiconducting properties of the passive film and the pitting corrosion resistance has been widely investigated, and the point defect density in the passive film is reported to be responsible for the passive film protectiveness and hence the pitting corrosion resistance.[11,16,17] Thus, in an effort to understand this relationship, the passive films of Fe20Cr and Fe20Cr1.1N alloys were investigated using Mott-Schottky analysis.

A capacitance of a space charge layer in the passive film was measured in 0.1 M H_2SO_4 solution at 1000 Hz,[18,21] and the Mott-Schottky curve was obtained as shown in Fig. 6(a). The polarization curves of the alloys measured at the same solution are displayed in Fig. 6(b), which present the stable passive potential regions of the alloys. The Mott-Schottky analysis was conducted on the passive film which was potentiostatically formed at 0.38 V_{SCE} for 4 hours, and the capacitance value was measured in the passive potential range with descending the applying potential. Mott- Schottky plots of the alloys exhibit positive slopes (dC_{SC}^{-2}/dV) in the potential range of 0-0.3 V_{SCE} (dashed line in Fig. 6(a)), which means the passive films of the two alloys have n-type semiconductivity. The n-type semiconductivity is due to the Fe_2O_3 component in the passive film.[16-18,20,21] In the n-type passive oxide film, the dominant and detectable donor species is an oxygen vacancy (V_O^{2+}),[16-18,20,21] and the N_D can be calculated from the Mott-Schottky plot, in accordance with the following relation between C_{SC} and E_{app}:

$$\frac{1}{C_{SC}^{\ 2}} = \frac{1}{C_{total}^2} - \frac{1}{C_H^2} = \left(\frac{2}{\varepsilon\varepsilon_o e N_D}\right)\left(E_{app} - E_{FB} - \frac{kT}{e}\right) \quad (1)$$

where ε is the dielectric constant of the oxide (15.6[28),29)]), ε_0 is the vacuum permittivity ($8.854'10^{-14}$ F cm^{-1}), e is the electron charge, E_{app} is the applied potential, and k is the Boltzmann constant. The measured capacitance value, C_{total}, is obtained from the relation of $C_{total}=1/\omega Z''$, where ω is the angular frequency (1000 Hz) and Z'' is the imaginary section of the specific impedance. C_{total} is a series combination of a double layer capacitance (Helmholtz layer capacitance, C_H) and a space charge layer capacitance (C_{SC}). Generally, the C_H value is much higher than the C_{SC} value thus, the measured capacitance (C_{total}) can be regarded as C_{SC}.[20)]

Based on Fig. 6(a), N_D values of the alloys were calculated and displayed in Fig. 6(c). The N_D value in the space charge layer of the passive films of Fe20Cr was 6.41x 10^{20} cm^{-3}, and that of Fe20Cr1.1N alloy was 1.12x10^{21} cm^{-3}. The V_O^{2+} is known to be the point defect in the passive film, and several reports have shown that lower V_O^{2+} concentration in the passive films reflect higher protectiveness of the passive film[16), 17), 20), 30), 31)]. Thus, the analysis results from the Mott-Schottky plot cannot provide satisfactory explanation of the improved pitting corrosion resistance of Fe20Cr1.1N alloy.

So far, the series of analyses on the passive films of Fe20Cr and Fe20Cr1.1N alloys formed in dilute H_2SO_4 solution revealed various characteristics of the passive films. The XPS observation provided several important results as follows: (1) the frame of the passive films formed on the two alloys in dilute sulfuric acid solution were mixed (Cr, Fe)-oxide. (2) The passive film with higher Cr fraction ([Cr]/[Cr+Fe]) was formed on the nitrogen-bearing Fe20Cr alloy than that of Fe20Cr alloy without nitrogen. (3) Nitrogen was incorporated into the passive film and enriched at the film-metal interface of Fe20Cr1.1N alloy. (4) The passive film on the Fe20Cr1.1N alloy was thinner than the Fe20Cr alloy without nitrogen. Galvanostatic reduction test confirmed again that the thinner passive film was formed on the nitrogen-bearing alloy in the H_2SO_4 solution. In addition, Mott-Schottky analysis provided the results that more defective passive film containing higher V_O^{2+} concentration was formed on the nitrogen- bearing alloy. The higher Cr content and incorporation of nitrogen in the passive film are known to contribute to the protectiveness of the passive film[9-11), 13), 14), 32)]. However, the observed features that the film of Fe20Cr1.1N alloy was thinner and more defective than that of Fe20Cr alloy were reported to have adverse effect to strengthening the protective ability of the passive film [9),15)-17),30)]. Thus, considering these results, the increased pitting corrosion resistance of Fe20Cr1.1N is considered primarily attributed to the chemical change of the passive film, that is the higher chromium and nitrogen content, and it can be concluded that the most important determining factor for strengthening the passive film protectiveness is the chemical structure than the film thickness and the defect density.

4. Conclusions

In this study, the resistance to the pitting corrosion resistance in dilute sulfuric acid of Fe20Cr and Fe20Cr1.1N alloy was evaluated by a potentiodynamic polarization test, and the characteristics of the passive films formed in the sulfuric acid solution were investigated through and an XPS and a galvanostatictest and Mott-Schottky analysis. From the investigation, the following results are obtained.

1. Nitrogen alloying was effective to enhance the resistance to pitting corrosion of Fe20Cr based alloy in sulfuric acid solutions containing chloride ion. This result demonstrated that the higher protective passive film formed on Fe20Cr1.1N alloy in the sulfuric acid solution.
2. The XPS analysis revealed that the passive films of the two alloys formed in sulfuric acid solution were composed of (Cr, Fe)-oxide, and the Cr cation fraction of Fe20Cr1.1N alloy was higher than that of Fe20Cr alloy. In addition, nitrogen was incorporated with the passive film of Fe20Cr1.1N alloy, and the maximum content of nitrogen was found at the film-metal interface.
3. From the XPS analysis and the galvanostatic reduction result, it was found that the passive film formed on the nitrogen-bearing alloy was thinner than that on Fe20Cr alloy without nitrogen.
4. Mott-Schottky analysis showed the passive film on Fe20Cr1.1N alloy had higher point defect density (oxygen vacancy density) than that of Fe20Cr alloy.

It was concluded that the higher protectiveness of the passive film on Fe20Cr1.1N alloy was mainly attributed to the higher chromium and nitrogen contents in the passive film than that of Fe20Cr alloy. In addition, the protectiveness of the passive film was primarily determined by the chemical composition change in comparison to the film thickness and defect density.

References

1. P. R. Levey and A. van Bennekom, *Corrosion*, **51**, 911 (1995).
2. M. Sumita, T. Hanawa and S. H. Teoh, *Mat. Sci. Eng. C-Mater.*, **24**, 753 (2004).
3. H. J. Grabke, *ISIJ Int.*, **36**, 777 (1996).
4. P. J. Uggowitzer, R. Magdowski and M. O. Speidel, *ISIJ*

Int., **36**, 901 (1996).
5. J. W. Simmons, *Mat. Sci. Eng. A-Struct.*, **207**, 159 (1996).
6. J. Menzel, W. Kirschner and G. Stein, *ISIJ Int.*, **36**, 893 (1996).
7. R. F. A. J.-Pettersson, *Corros. Sci.*, **41**, 1639 (1999).
8. K. H. Lo, C. H. Shek and J. K. L. Lai, *Mat. Sci. Eng. R*, **65**, 39 (2009).
9. I. Olefjord and L. Wegrelius, *Corros. Sci.*, **38**, 1203 (1996).
10. A. S. Vanini, J.-P.Audouard and P. Marcus, *Corros. Sci.*, **36**, 1825 (1994).
11. H. Ha, H. Jang and H. Kwon, *Corros. Sci.*, **51**, 48 (2009).
12. M. K. Lei and X. M. Zhu, *J. Electrochem. Soc.*, **152**, B291 (2005).
13. R. D. Willenbruch, C. R. Clayton, M. Oversluizen, D. Kim and Y. Lu, *Corros. Sci.*, **31**, 179 (1990).
14. C.-O. A. Olsson, *Corros. Sci.*, **37**, 467 (1995).
15. Y. Fu, X. Wu, E.-H. Han, W. Ke, K. Yang and Z. Jiang, *Electrochim. Acta*, **54**, 4005 (2009).
16. M. Metikos-Hukovic, R. Babic, Z. Grubac, Z. Petrovic and N. Lajci, *Corros. Sci.*, **53**, 2176 (2011).
17. S. Ningshen, U. K. Mudali, V. K. Mittal and H. S. Khatak, *Corros. Sci.*, **49**, 481 (2007).
18. S. Ahn and H. Kwon, *J. Electroanal. Chem.*, **579**, 311 (2005).
19. K. N. Goswami and R. W. Staehle, *Electrochim. Acta*, **16**, 1895 (1971).
20. H.-Y. Ha and H.-S. Kwon, *J. Electrochem. Soc.*, **159**, C416 (2012).
21. H.-Y. Ha, T.-H. Lee and S.-J. Kim, *Electrochim. Acta*, **80**, 432 (2012).
22. T. Massoud, V. Maurice, L. H. Klein and P. Marcus, *J. Electrochem. Soc.*, **160**, C232 (2013).
23. H. Luo, X. G. Li, C. F. Dong and K. Xiao, Surf. *Interface Anal.*, **45**, 793 (2013).
24. A. Kocijan, C. Donik and M. Jenko, *Corros. Sci.*, **49**, 2083 (2007).
25. C. M. Abreu, M. J. Cristobal, P. Merino, X. R. Novoa, G. Pena and M. C. Perez, *Electrochim. Acta*, **53**, 6000 (2008).
26. N. Sato, K. Kudo and T. Noda, *Electrochim. Acta*, **16**, 1909 (1971).
27. N. Sato, K. Kudo and R. Nishimura, *J. Electrochem. Soc.*, **123,** 1419 (1976).
28. A. M. P. Simoes, M. F. S. Ferreira, B. Rondot and M. Da Cunha Belo, *J. Electrochem. Soc.*, **137**, 82 (1990).
29. E. Cho, H. Kwon and D. D Macdonald, *Electrochim. Acta*, **47**, 1661 (2002).
30. S. Ahn, H. Kwon and D. D. Macdonald, *J. Electrochem. Soc.*, **152**, B482 (2005).
31. N. Li, Y. Li, S. Wang and F. Wang, *Electrochim. Acta*, **52**, 760 (2006).
32. A. Shahryari, S. Omanovic and J. Z. Szpunar, *Mat. Sci. Eng. C-Mater.*, **28**, 94 (2008).